Fluoxetine Induces Input-Specific Hippocampal Dendritic Spine Remodeling Along the Septotemporal Axis in Adulthood and Middle Age

Kathleen McAvoy,[1,2,3] Craig Russo,[1,2,3] Shannen Kim,[1,2,3] Genelle Rankin,[1,2,3] and Amar Sahay[1,2,3]*

ABSTRACT: Fluoxetine, a selective serotonin-reuptake inhibitor (SSRI), is known to induce structural rearrangements and changes in synaptic transmission in hippocampal circuitry. In the adult hippocampus, structural changes include neurogenesis, dendritic, and axonal plasticity of pyramidal and dentate granule neurons, and dedifferentiation of dentate granule neurons. However, much less is known about how chronic fluoxetine affects these processes along the septotemporal axis and during the aging process. Importantly, studies documenting the effects of fluoxetine on density and distribution of spines along different dendritic segments of dentate granule neurons and CA1 pyramidal neurons along the septotemporal axis of hippocampus in adulthood and during aging are conspicuously absent. Here, we use a transgenic mouse line in which mature dentate granule neurons and CA1 pyramidal neurons are genetically labeled with green fluorescent protein (GFP) to investigate the effects of chronic fluoxetine treatment (18 mg/kg/day) on input-specific spine remodeling and mossy fiber structural plasticity in the dorsal and ventral hippocampus in adulthood and middle age. In addition, we examine levels of adult hippocampal neurogenesis, maturation state of dentate granule neurons, neuronal activity, and glutamic acid decarboxylase-67 expression in response to chronic fluoxetine in adulthood and middle age. Our studies reveal that while chronic fluoxetine fails to augment adult hippocampal neurogenesis in middle age, the middle-aged hippocampus retains high sensitivity to changes in the dentate gyrus (DG) such as dematuration, hypoactivation, and increased glutamic acid decarboxylase 67 (GAD67) expression. Interestingly, the middle-aged hippocampus shows greater sensitivity to fluoxetine-induced input-specific synaptic remodeling than the hippocampus in adulthood with the stratum-oriens of CA1 exhibiting heightened structural plasticity. The input-specific changes and circuit-level modifications in middle-age were associated with modest enhancement in contextual fear memory precision, anxiety-like behavior and antidepressant-like behavioral responses. © 2015 Wiley Periodicals, Inc.

INTRODUCTION

The last decade has seen considerable progress investigating how SSRIs such as fluoxetine exert their antidepressant effects (Berton and Nestler, 2006; Castren and Hen, 2013; Vialou et al., 2013). In adult rodents, chronic fluoxetine induces changes in hippocampal gene expression (Conti et al., 2007; Miller et al., 2008; Patricio et al., 2015), as well as widespread circuit remodeling and structural rearrangements in the hippocampus (Pittenger and Duman, 2008; Bessa et al., 2009; Castren and Hen, 2013). These include augmentation of adult hippocampal neurogenesis (proliferation of progenitors and activation of neural stem cells, as well as enhanced survival and maturation of adult-born dentate granule neurons) (Malberg et al., 2000; Santarelli et al., 2003; Encinas et al., 2006; Sahay et al., 2007; Wang et al., 2008; David et al., 2009) and changes in dendritic complexity and dendritic spines (Hajszan et al., 2005; Wang et al., 2008; Bessa et al., 2009; Huang et al., 2012; Rubio et al., 2013). In addition to these structural changes, chronic fluoxetine treatment also induces a de-differentiation-like phenotype of mature dentate granule neurons (Kobayashi et al., 2010), modulates mossy fiber synaptic transmission (Kobayashi et al., 2008, 2010, 2012; Stagni et al., 2013), and affects excitatory and inhibitory synaptic transmission in the hippocampus (Stewart and Reid, 2000; Moutsimilli et al., 2005; Airan et al., 2007; Kobayashi et al., 2008, 2012; Reines et al., 2008; Luscher et al., 2011; Mendez et al., 2012; Rubio et al., 2013; Stagni et al., 2013). Many of these circuit-wide rearrangements and changes in neural activity are mediated by a plethora of growth factors whose expression is upregulated by chronic fluoxetine treatment (Schmidt and Duman, 2007). Importantly, some of these changes such as enhancing adult hippocampal neurogenesis or increased expression of brain derived neurotrophic

factor have been causally implicated in the antidepressant-like actions of chronic fluoxetine or been shown to be sufficient to produce antidepressant-like effects (Shirayama et al., 2002; Santarelli et al., 2003; Li et al., 2008; David et al., 2009; Surget et al., 2011; Mateus-Pinheiro et al., 2013; Miller and Hen, 2014; O'Leary and Cryan, 2014; Walker et al., 2014; Wu and Hen, 2014; Hill et al., in press).

Although these studies have advanced our knowledge about how changes in hippocampal connectivity and circuitry may contribute to the therapeutic actions of chronic fluoxetine, we know surprisingly little about whether fluoxetine's effects on synaptic remodeling show input-specificity or vary along the septotemporal axis. This is important to address as considerable evidence suggests that information processing in hippocampal neurons is reliant on integration of diverse range of inputs that are segregated by laminae along the dendritic tree (Spruston, 2008). For example, dendritic spines of CA1 pyramidal neurons in stratum radiatum (SR) and stratum oriens (SO) receive indirect excitatory inputs from the entorhinal cortex CA3 via the schaffer collaterals, whereas dendritic spines of CA1 pyramidal neurons in stratum lacunosum moleculare (SLM) receive direct excitatory inputs from the entorhinal cortex via the temporoammonic pathway. Furthermore, the excitability and threshold for plasticity of apical and basal dendrites in stratum radiatum and stratum oriens, respectively are different (Spruston, 2008). In the DG, the inner molecular layer is primarily host to inputs from mossy cells and supramammillary nuclei (Amaral et al., 2007), whereas the outer molecular layer receives inputs from the entorhinal cortex (Leranth and Hajszan, 2007).

Serotonin receptors have differential effects on synaptic plasticity through augmentation and inhibition of NMDA-receptor based plasticity, AMPA receptor trafficking, post-synaptic calcium signaling, and regulation of synaptic adhesion molecules (Lesch and Waider, 2012). These fundamental mechanisms of plasticity that are thought to underlie learning and memory are associated with strengthening and weakening of synapses and parallel increases and decreases in dendritic spine size (Bosch and Hayashi, 2012). Expression of serotonin receptors varies across laminae, cell type, and region (Berumen et al., 2012), therefore enabling modification of plasticity at a sub-cellular, cellular, and circuit level. Although a few studies have examined effects of fluoxetine treatment on dendritic spines in apical dendrites of CA1 (Huang et al., 2012) (adult male mice), (Hajszan et al., 2005) (adult ovariectomized female rats), (Rubio et al., 2013) (adult male rats), (Chen et al., 2008) (adult male rats, imipramine), or proximal and apical dendrites of dorsal CA3 (Bessa et al., 2009), there are no studies to date that have systematically examined how dendritic spines within different molecular layers of DG and CA1 in dorsal and ventral hippocampus change in response to chronic fluoxetine. Furthermore, since hippocampal functions are governed by their intrinsic and extrinsic connectivity along the septotemporal axis (Fanselow and Dong, 2010; Strange et al., 2014), it is important to ascertain if chronic fluoxetine treatment differentially affects laminae-specific dendritic inputs as a function of dorsal and ventral location.

A second question we sought to address in this study is how fluoxetine-induced circuit remodeling and changes in neuronal activity vary during aging. Remarkably, only a handful of studies have examined how hippocampal circuitry is affected by chronic fluoxetine in middle- aged rodents, a stage that corresponds to humans in the age range of 38 to 50 years (Miller et al., 2007) and when levels of adult hippocampal neurogenesis are comparable between the two species (Eriksson et al., 1998; Knoth et al., 2010; Snyder et al., 2011; Snyder and Cameron, 2012; Spalding et al., 2013). Although several studies have consistently found the lack of a pro-neurogenic effect of chronic fluoxetine in middle-aged rodents (Cowen et al., 2008; Couillard-Despres et al., 2009; Guirado et al., 2012), the effects of chronic fluoxetine on dendritic spines in the DG or CA1 or terminally differentiated state of mature dentate granule neurons in middle-aged rodents is not known.

Here, we sought to bridge these gaps in our knowledge by addressing how chronic fluoxetine treatment affects circuit-rearrangements and input-specific dendritic spine remodeling in DG and CA1 neurons across the septotemporal axis in adulthood and in middle age. We compared the effects of chronic fluoxetine on adult hippocampal neurogenesis, granule neuron maturation state, markers of excitatory and inhibitory neurotransmission, and activity of the DG and CA3 in adulthood and middle age. Using a transgenic mouse line in which mature dentate granule neurons (older than 4 weeks of age) and CA1 pyramidal neurons are genetically labeled with GFP (Feng et al., 2000; Vuksic et al., 2008), we systematically quantified the density and distribution of dendritic spines in these two neuronal populations across different molecular layers of DG and CA1, as well as the distribution of mossy fiber terminal size (Supporting Information Figure 1). Our studies reveal that while specific circuit-wide rearrangements induced by chronic fluoxetine, such as augmentation of adult hippocampal neurogenesis are lost in middle age, others, such as reduced activity-induced gene expression and loss of markers of maturation, persist in middle age. In addition, in adulthood chronic fluoxetine treatment induced an increase in dendritic spine density only in the dorsal stratum oriens of CA1, whereas in middle age an increase in dendritic spine density was seen throughout the septotemporal axis in stratum oriens, as well as in ventral stratum radiatum of CA1. In middle age, synaptic remodeling was also indicated by a shift in spine size distribution in dendritic regions of both the DG and CA1. These input-specific changes in dendritic spines induced by chronic fluoxetine may differentially impact synaptic transmission and cognate learning processes associated with basal dendrites of CA1.

As a first step toward this goal, we assessed the impact of chronic fluoxetine treatment in middle-age on hippocampal dependent learning and memory (contextual fear conditioning and memory precision), anxiety-like and depression-like behaviors. Chronic fluoxetine treatment did not affect acquisition of contextual fear or memory one day following training. However, chronic fluoxetine treatment modestly enhanced long term-contextual fear memory precision at 2 weeks post-training. Chronic fluoxetine treatment also increased anxiety-like behaviors in the open field, elevated plus maze and
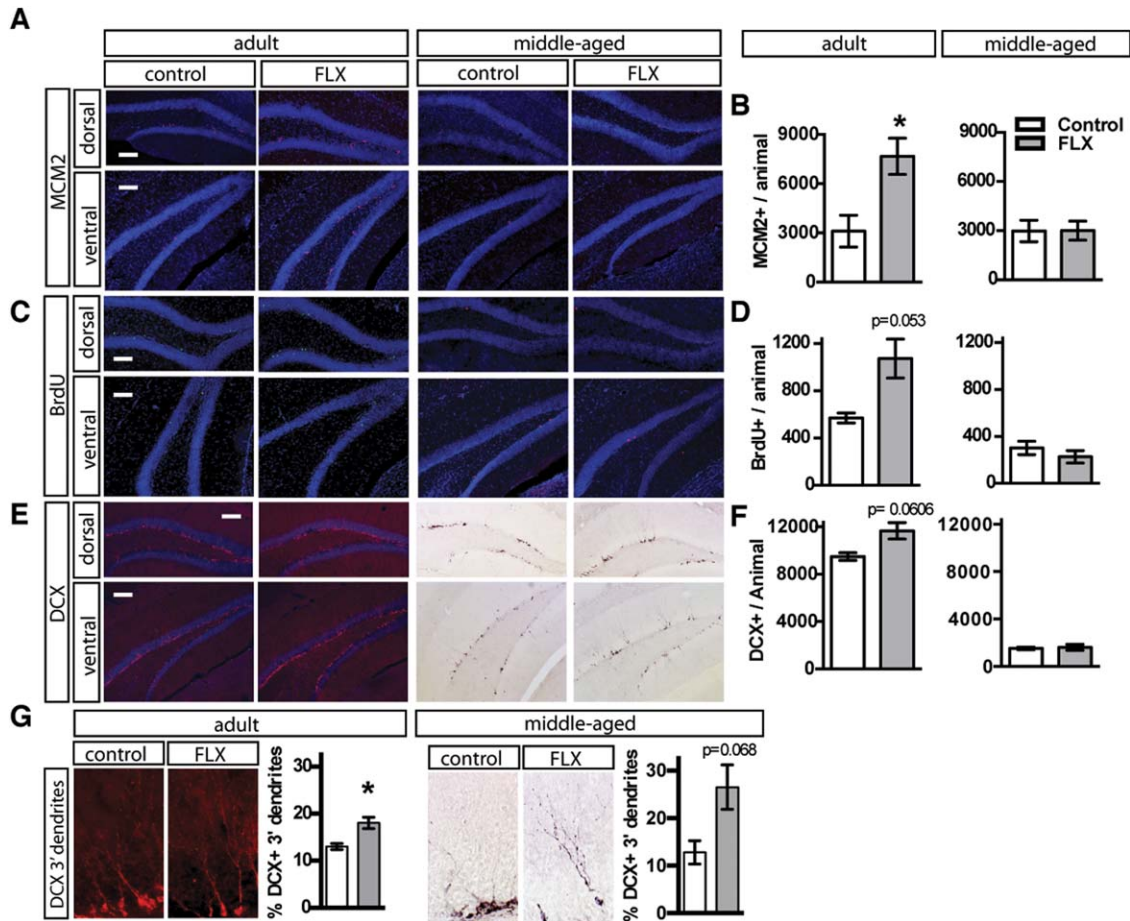
FIGURE 1. Fluoxetine treatment increases progenitor proliferation and survival of adult-born neurons in adult but not middle-aged mice. A. Representative MCM2 immunostained coronal hippocampal sections of adult and middle-aged mice following 4 weeks of fluoxetine treatment. B. Fluoxetine-treated (18 mg/kg/day for 28 days) adult mice, but not fluoxetine-treated middle-aged mice, show increased granule cell layer MCM2 positive cells. Adult $n = 3$ (VEH), 5 (FLX) mice per group, $P = 0.0315$, middle-aged $n = 3$ (VEH), 4 (FLX), $P = 0.9846$). C. BrdU (150 mg/kg) was administered i.p. 1 week after the start of Fluoxetine treatment. Representative BrdU immunostained coronal hippocampal sections of adult and middle-aged mice 3 weeks following BrdU injection. D. Fluoxetine-treated adult mice, but not fluoxetine-treated middle-aged mice, show increased granule cell layer BrdU positive cells. (Adult $n = 3$ (VEH), 4 (FLX) mice per group, $P = 0.0530$, middle-aged $n = 3$ (VEH), 4 (FLX), $P = 0.3868$). E. Representative DCX immunostained coronal hippo-campal sections of adult and middle-aged mice after 4 weeks of Fluoxetine treatment. Middle-aged mice exhibit a dramatically reduced population of young adult-born neurons. F. Adult mice receiving fluoxetine show a trend toward increased young adult-born neurons, whereas fluoxetine treatment in middle-aged mice does not change the population of young adult-born neurons. (Adult $n = 3$ (VEH), 5 (FLX) mice per group, $P = 0.0606$, middle-aged $n = 3$ (VEH), 4 (FLX), $P = 0.8092$). G. High magnification image of DCX immunostained young adult-born neurons with tertiary dendrites. Both adult and middle-aged mice treated with fluoxetine show an increased percentage of the DCX positive population with tertiary dendrites. (Adult $n = 3$ (VEH), 5 (FLX) mice per group, $P = 0.0247$, middle-aged $n = 3$ (VEH), 4 (FLX), $P = 0.0680$). Results are expressed as mean ($\pm$SEM). $P < 0.05$*. Scale bar: 100 µM. [Color figure can be viewed in the online issue, which is available at wileyonlinelibrary.com.]

light-dark tests but not in the novelty suppressed feeding paradigm. In the forced swim test, we observed a modest decrease in immobility in the fluoxetine group that is typically construed as an antidepressant-like behavioral response. However, no effect was seen on anhedonia as assessed in the sucrose preference test. Further experiments are needed for systematic assessment of how chronic fluoxetine treatment affects synaptic transmission, cognition and mood across the lifespan and also under conditions of stress when the behavioral effects of fluoxetine may be most therapeutically relevant.

MATERIALS AND METHODS

Mouse Lines and Animal Care

Thy1-GFP (m-Line) mice were purchased from Jackson Labs (http://www.jax.org/index.html; strain 007788) and were maintained by crossing to C57BL/6J (strain 000664) also purchased from Jackson Labs. Adult (4–5 months old) and middle-aged (10–11 months old) Thy1-GFP female mice were

used for experiments. Mice were housed four to five per cage in a 12 h (7:00 A.M. to 7:00 P.M.) light/dark colony room at 22 to 24 °C with ad libitum access to food and water. All animals were handled and experiments were conducted in accordance with procedures approved by the Institutional Animal Care and Use Committee at the Massachusetts General Hospital in accordance with NIH guidelines.

Immunohistochemistry

Mice were anaesthetized with ketamine or xylazine (100 and 7 mg kg^{-1} body weight, respectively) and transcardially perfused (with cold saline, followed by 4% cold paraformaldehyde in PBS). Brains were postfixed overnight in 4% paraformaldehyde at 4 °C, then cryoprotected in 30% sucrose and stored at 4 °C. Coronal serial sections (35 μm) were obtained using a Leica cryostat in six matched sets (one in six) and stored in PBS with 0.01% sodium azide at 4 °C. For BrdU and MCM2 immunohistochemistry, sections (one set) were mounted onto SuperFrost Plus charged glass slides. Sections were subjected to antigen retrieval in 10 mM citrate buffer (pH 6) using a boiling protocol. After cooling to room temperature, sections were rinsed three times in PBS and blocked in PBS with 0.3% Triton X-100 and 10% normal donkey serum (NDS) for 2 h at room temperature. Incubation with primary antibodies (rat anti-BrdU antibody 1:100 dilution, Serotec, mouse, anti-MCM2 antibody, BD Biosciences, 1:500) was carried out at 4 °C overnight. Fluorescent-label-coupled secondary antibodies (Jackson ImmunoResearch) were used at a final concentration of 1:200 in PBS:glycerol. To label Calbindin (mouse, 1:5,000, Swant), ZnT3 (rabbit, Synaptic Systems, 1:2,000), GAD67 (mouse, EMD Millipore, 1:2,000), DCX (goat, 1:500, Santa-Cruz Biotechnology), Bassoon (rabbit, Abcam, 1:500), and cfos (rabbit, Calbiochem, 1:10,000) floating sections were used. Briefly, sections were washed in PBS, blocked in PBS buffer containing 0.3% Triton X-100 and 10% NDS, and incubated in primary antibodies overnight, with shaking at 4 °C. The next day, sections were washed three times in PBS and incubated with fluorescent-label-coupled secondary antibodies (Jackson ImmunoResearch) for 2 h at room temperature. For DCX immunohistochemistry (adult sections), floating sections were first quenched to remove endogenous peroxidase activity (with 1% H2O2 in 1:1 PBS:methanol). Sections were then washed in PBS, blocked (in PBS containing 0.3% Triton X-100 and 10% NDS) and incubated with primary antibody overnight at 4 °C (DCX, goat, 1:2,000, SantaCruz Biotechnology). Following washes in PBS, sections were incubated with horse-radish-peroxidase-coupled, biotinylated secondary antibodies for 2 h. Following incubation with ABC solution (Vector Labs) for 1 h, the color reaction was carried out using a DAB kit (Vector Labs).

For BrdU, MCM2, and DCX analysis, positive cells in the granule cell layer and subgranule zone were counted manually along the dorsal to ventral axis of the dentate gyrus (one set of six; nine sections). Dorsal and ventral sections were defined according to the Paxinos and Franklin (1997) atlas (dorsal

Bregma -0.9 to -2.1; ventral Bregma -2.7 to -3.88). Summing the counted cells and multiplying by 6 yields the total per animal. To analyze the maturation state of the immature neurons, DCX-positive cells with tertiary dendrites were counted and expressed as a percentage of the total DCX population. For cfos analysis, positive cells in the granule cell layer and CA3 pyramidal layer were counted manually along the dorsal to ventral axis of the hippocampus (one set of six; three sections each dorsal, intermediate, and ventral regions). For Calbindin, Bassoon, GAD67, and ZnT3 quantification, images were captured at 20× magnification. At least three images per region per animal were analyzed using ImageJ. Intensity quantification was performed on ZnT3 labeling in the mossy fiber termination region in stratum lucidum in CA3. For calbindin labeling, intensity quantification was performed on selected regions from the DG molecular layer (ML), granule cell layer (GCL), and the mossy fiber region in the stratum lucidum of CA3 (CA3). For Gad67 labeling, intensity quantification was performed on selected regions from the DG granule cell layer (GCL), hilus, and the pyramidal cell layer in CA3. For Bassoon labeling, intensity quantification was performed on selected regions from the DG outer molecular layer (OML), hilus, and the mossy fiber terminals in stratum lucidum in CA3. Intensity was calculated from a highlighted region of interest using the mean intensity function and normalized to background.

Image Analysis of Dendritic Spines

For quantification of dendritic spines, confocal z-stack images were acquired using a Nikon A1R Si confocal laser, a TiE inverted research microscope, and NIS Elements software. Imaging was performed using a 60× objective, plus 1.5× optical zoom, and 6× digital zoom. For spine imaging, confocal 2.1 μM z-stacks (2,048 resolutions) with 0.3 μM step size were taken centered on dendritic segment. z-stacks were flattened using the maximum intensity projection, and flattened images were quantified using ImageJ. For spine density, spines were counted manually for at least 80 μM of dendritic length per region per mouse. The Edge fitter plugin (www.ghoshlab.org) was used to measure head diameter (at the widest point of the spine head) while length was measured manually from dendrite to the furthest point of the spine head. Hundred to 500 spines were analyzed per region per mouse to calculate spine size distribution. All imaging and quantification were performed by an investigator blind to treatment.

Image Analysis of Mossy Fiber Terminals

A Nikon A1R Si confocal laser, a TiE inverted research microscope, and NIS Elements software were used to capture z-stacks for Mossy fiber terminal (MFT) imaging using a 60x objective as we recently published (Ikrar et al., 2013). Images were acquired as 15 μM z-stacks with a step size of 0.5 μM. Area of individual MFTs was assessed at the widest point in the z-stack using ImageJ MaxEntropy thresholding, followed by unbiased area selection with the tracing tool. MFTs area

was analyzed for >100 individual MFTs per region per mouse to calculate the cumulative percentage of spines at each size or smaller.

BrdU Injections and Fluoxetine Administration

Fluoxetine (Sigma-Aldrich Corporation, St Louis, MO) was made available ad libitum in the drinking water. The concentration of each drug was determined from the average daily water consumption per cage (determined per mouse from a prior pilot study), and the total body weight per cage of mice to achieve a dose of 18 mg/kg/mouse/day. Treatment continued for 28 days, with fluoxetine solution replaced every third day. To assess the survival of adult-born neurons in the dentate gyrus, BrdU was administered on day 7 of Fluoxetine treatment via intraperitoneal injection, in 0.9% NaCl at 150 mg/kg body weight.

Behavioral Testing

Behavioral tasks were performed in the following order: open field (day 1), light-dark choice test (day 2), elevated plus maze (day 3), forced swim test (day 4,5), Novelty suppressed feeding test (day 6), sucrose preference test (day 9, 10, 11), and contextual fear conditioning test (day 12–15, day 29).

Open Field

Mice were kept in a quiet, darkened room for at least 1 h without food before the test. Motor activity over 60 min was quantified in four Plexiglas open-field boxes of 41 × 41cm (Kinder Scientific) with 16 sets of double stacked pulse-modulated infrared photobeams equally spaced on every wall (128 total) to record x–y–z ambulatory movements. The software defined grid lines that divided each open field into center and surround regions, with the periphery consisting of the 10 cm closest to the wall around the entire perimeter. Dependent measures were the distance traveled in the center, time spent in the center, and distance traveled in the center divided by total distance traveled (percentage distance). Overall motor activity was quantified as the total distance traveled (in cm).

Light–Dark Choice Test

The light/dark test was conducted in the open-field chamber as above, but with a dark plastic box that is opaque to visible light but transparent to infrared covering one-half of the chamber area, thus creating dark and light compartments of equal size. An opening at floor level in the center of one wall of the dark compartment allowed passage between the light and dark compartments. The light compartment was brightly illuminated. Mice were kept in a quiet, darkened room for at least 1 h before the test without food. Between each trial, the whole apparatus was cleaned. At the beginning of the test, the mouse was placed in the dark compartment and allowed to freely explore both compartments for 10 min. Ambulation distance and time spent in the dark and the light compartments were recorded.

Elevated Plus Maze Test

The elevated plus maze consisted of black Plexiglass apparatus with four arms (16 cm long and 5 cm wide) set in a cross from a neutral central square (5 cm × 5 cm) placed 1 m above the floor. Two opposing arms were delimited by vertical walls (closed arms), while the two other opposing arms had unprotected edges (open arms). Mice were placed in the center and their behavior was recorded for 5 min via a video camera system (ViewPoint, Lyon, France) located above the maze. Cumulative time spent in the open and closed arms, and entries into the open and closed arms, were scored manually by investigators blind to the treatment conditions. An arm visit was recorded when the mouse moved the forepaws into the arm.

Forced-Swim Test

Mice were placed in transparent plastic buckets (17 cm diameter; 25 cm deep) filled with 23 to 26 °C water for 6 min and the animal's behavior was recorded using an automated video-tracking system. Testing was performed over 2 consecutive days with the first day serving the purpose of pre-exposure. Mobility (swimming and climbing behaviors) on the second day was analyzed using View-Point Life Sciences software.

Sucrose Preference Test

Mice were acclimated to individual housing and to two water bottles for 48 h before the start of testing. At day 1 of testing, just before the start of the dark cycle, mice were given two water bottles with sipper tubes containing water or a 4% sucrose solution. Volume of the sucrose solution and water consumed was determined after the dark cycle (12 h) and after the light cycle (24 h). This paradigm was repeated with 2% (day 2) and 1% (day 3) sucrose. Sucrose preference was calculated as: volume sucrose/(total volume sucrose + water).

Novelty-Suppressed Feeding Test

Mice were food deprived in their home cages for 24 to 26 h before testing. The testing apparatus consisted of a plastic arena (45 cm long, 15 cm high, and 30 cm wide) whose floor was covered with an ~2 cm depth of wood-chip bedding. A single food pellet (familiar laboratory mouse chow) was placed on a circular piece of white filter paper (12 cm in diameter) positioned in the center of the arena. The test began with a mouse being placed in a corner of the arena, and the latency to approach the pellet and begin feeding was recorded (for a maximum time of 15 min). Testing was carried out under bright light conditions. Each mouse was weighed before food deprivation and just before testing to assess changes in body weight. Each group (VEH and FLX) lost ~9 to 10% body weight. Immediately after the test, each mouse was transferred to its home cage, and the latency to consume food from the overhead rack was measured (within 5 min). When appropriate, survival analysis was performed, and statistical differences

between the latencies were determined using the Log rank Mantel-Cox test.

Contextual Fear Conditioning

Conditioning was conducted in Coulbourn Habitest fear conditioning chambers with clear front and back Plexiglas walls, aluminum side walls, and stainless-steel bars as a floor. The chamber was lit from above with a light, ventilated with a fan, and encased by a sound-dampening cubicle. On the days of testing, mice were brought out of the vivarium and allowed to habituate for an hour outside the testing room before starting the experiment. Mouse behavior was recorded by digital video cameras mounted above the conditioning chamber. Freezeframe and Freezeview software (Actimetrics) were used for recording and analyzing freezing behavior, respectively. For the training context, the fan and lights were on, stainless-steel bars were exposed, and ethanol was used as an olfactory cue. Mice were brought into the testing room in a standard housing cage. The contextual fear conditioning protocol entailed delivery of a single 2 s footshock of 0.7 mA, 180 s after placement of the mouse in the training context. The mouse was taken out 20 s after termination of the footshock and returned to its home cage. Freezing levels were quantified over the initial 180 s before the shock. This protocol was repeated on days 1 to 3. On day 4, animals were exposed to the training context (in which they did not receive a shock) or a novel context for 3 min. Animals were counterbalanced for order of exposure, with the second exposure occurring 2 h following the initial test. For the novel context, the stainless-steel grid floor was covered with a plastic panel. Two of the chamber walls were covered using plastic inserts with black and white shapes. Mice were brought into the testing room in cardboard buckets. Freezing levels in both contexts were calculated over the first 180 s. Fourteen days following test day 4 (i.e. day 18) mice were exposed to the training and safe (novel) contexts in a counterbalanced design.

Statistical Analysis

Statistical analysis was carried out using GraphPad Prism software. Statistical significance ($P < 0.05$) was assessed by unpaired two-tailed Student's t-tests. *$P < 0.05$; **$P < 0.01$. Because of small sample sizes, we also performed two additional statistical tests (t-test with Welch's correction for unequal variances and the Mann-Whitney test) for all experiments in Figures 1–7 and which can be found in Supporting Information Table 1. Spine and mossy fiber terminal distribution were assessed using Komolgrov-Smirnoff tests with significance at $P < 0.0001$.

RESULTS

Chronic, but not subchronic, fluoxetine treatment has been shown to stimulate proliferation of neural progenitors and enhance the survival and maturation of adult-born neurons in the DG of adult rodents. We asked if these proneurogenic changes were also seen in middle-aged female mice. Adult (4 months) or middle-aged (10 months) female C57Bl/6J mice were administered fluoxetine in the drinking water for 28 days. The mice were given a pulse of BrdU (5-bromo-2'-deoxyuridine) after 1 weeks of treatment. We then examined progenitor proliferation in the DG by immunohistochemistry for Minichromosome maintenance protein 2 (MCM2), a cell proliferation marker. Adult, but not middle-age mice, showed a robust elevation in proliferation (Figure 1A-B, Adult $n = 3$ (VEH), 5 (FLX), $P = 0.0315$, middle-aged (MA) $n = 3$ (VEH), 4 (FLX) $P = 0.9846$). Analysis of BrdU-positive cells in the granule cell layer 3 weeks following pulse suggested an enhancement in survival of adult-born cells in adult, but not middle-aged mice (Figure 1C-D, adult $n = 3$ VEH, 4 FLX $P = 0.0530$, middle-aged (MA) $n = 3$ (VEH), 4 (FLX), $P = 0.3868$). Consistent with these effects seen in adulthood but not in middle-age, chronic fluoxetine treatment induced a trend toward an increase in the total number of young adult-born neurons as assessed by doublecortin (DCX) immunohistochemistry (Figure 1E-F, adult $n = 3$ (VEH), 5 (FLX). $P = 0.0606$, middle-aged (MA) $n = 3$ (VEH), 4 (FLX), $P = 0.8092$). However, a subtle effect on the maturation of young adult-born neurons, indicated by an increased percentage of DCX-positive cells showing tertiary dendrites, persisted as a trend-level effect in middle-aged mice treated with fluoxetine (Figure 1G, adult $n = 3$ (VEH), 5 (FLX), $P = 0.0247$, middle-aged (MA) $n = 3$ VEH, 4 FLX $P = 0.0680$).

Within the DG, chronic fluoxetine treatment also promotes loss of markers of differentiation of dentate granule neurons, such as calbindin, which is accompanied by reversal of physiological maturation, reduced mossy fiber synaptic facilitation and reduced activity-induced gene expression in the DG (Kobayashi et al., 2010). Following 4 weeks of chronic fluoxetine, calbindin expression was decreased in granule cell layer (GCL) dorsally in adulthood and ventrally in middle age and in both dorsal and ventral molecular layer (ML) in middle-aged mice (Figure 2A-C, Adult $n = 3$ (VEH), 5 (FLX) mice per group, dML $P = 0.1379$, vML $P = 0.4369$, dGCL $P = 0.0167$, vGCL $P = 0.0724$, dCA3 $P = 0.1248$, vCA3 $P = 0.5829$; middle-aged (MA) $n = 3$ (VEH), 4 (FLX), dML $P = 0.0245$, vML $P = 0.0173$, dGCL $P = 0.0790$, vGCL $P = 0.0036$, dCA3 $P = 0.4551$, vCA3 $P = 0.2927$). To determine if neuronal activity was altered in the DG and CA3 sub regions, we examined expression of the activity dependent immediate early gene, c-fos. Chronic fluoxetine treatment profoundly decreased expression of c-fos in the dorsal and ventral DG and CA3 of adult and middle-aged mice (Figure 3 A-B, adult $n = 3$ (VEH), 5 (FLX), dDG $P = 0.0008$, vDG $P = 0.0326$, dCA3 $P = 0.0055$, vCA3 $P = 0.0067$, MA $n = 3$ (VEH), 4 (FLX) dDG, $P = 0.0009$, vDG $P = 0.0552$, dCA3 $P = 0.0052$).

Alterations in excitation-inhibition balance in the dentate gyrus are often associated with reductions in calbindin expression. Moreover, recent studies have found that chronic
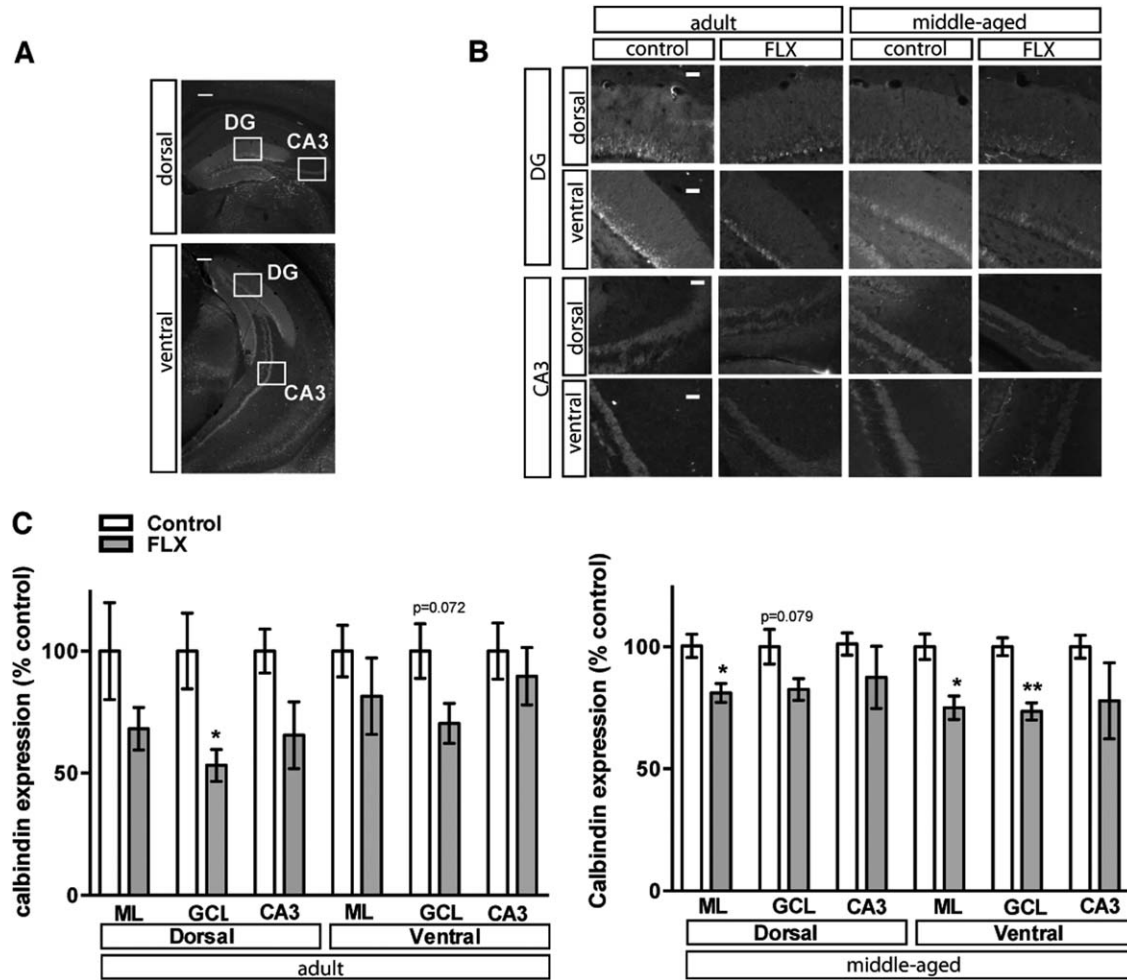
FIGURE 2. Fluoxetine treatment decreases calbindin expression in the DG of adult and middle-aged mice. A. Representative calbindin immunostained dorsal and ventral coronal hippocampal sections of adult control mice. Boxes indicate approximate locations of high magnification micrographs in B. B. Representative high magnification images of calbindin immunostained dorsal and ventral DG and CA3 from adult and middle-aged mice. C. Calbindin labeling intensity, calculated from six hemisections per mouse, is decreased in select regions in adult and middle-aged hippocampus following 4 weeks of fluoxetine treatment (18 mg/kg/day). The mean intensity (±SEM) of calbindin labeling is expressed as percentage of control labeling in the respective region in age-matched controls. *$P < 0.05$; **$P < 0.01$. Scale bar: 200 μM (A), 50 μM (B).

fluoxetine treatment modulates GABAergic transmission and induces expression of the GABA synthesizing enzyme, glutamic acid decarboxylase 67 (GAD67) (Luscher et al., 2011; Stagni et al., 2013; Guirado et al., 2014). Based on these observations, we examined GAD67 levels in the dorsal and ventral dentate gyrus of adult and middle-aged mice following chronic fluoxetine treatment. Adult mice showed a trend for an increase in GAD67 expression in the granule cell layer of dorsal DG and dorsal CA3 with no changes observed in ventral DG and CA3. Consistently, middle-aged mice showed a dramatic upregulation of GAD-67 in the granule cell layer of the dorsal DG and dorsal hilus (Figure 4A-C, adult $n = 3$ (VEH), 5 (FLX), dGCL $P = 0.0539$, dCA3 $P = 0.0757$, MA $n = 3$ (VEH), 4 (FLX) dGCL $P = 0.031$, dHilus $P = 0.0309$, vCA3 $P = 0.0878$). Together, these data suggest that chronic fluoxetine treatment induces dematuration of the granule cell

layer and increases GAD67 expression in both adulthood (trend) and in middle age, but does not stimulate adult hippocampal neurogenesis in middle age.

To determine if chronic fluoxetine treatment induced changes in dendritic spines in different laminae of the DG, we examined dendritic spine density of mature dentate granule neurons in the dorsal and ventral DG of adult and middle-aged mice. Hippocampal sections obtained from cohorts of 4 months and 10 months old transgenic Thy-1 GFP mice that were treated with 4 weeks of fluoxetine or vehicle were analyzed by confocal microscopy. Chronic fluoxetine treatment did not affect density or distribution of dendritic spines in the inner molecular layer or outer molecular layer of the dorsal or ventral DG of adult mice (Figure 5A-B). In middle-aged mice, chronic fluoxetine treatment increased the density of dendritic spines in the outer molecular layer of the dorsal DG,
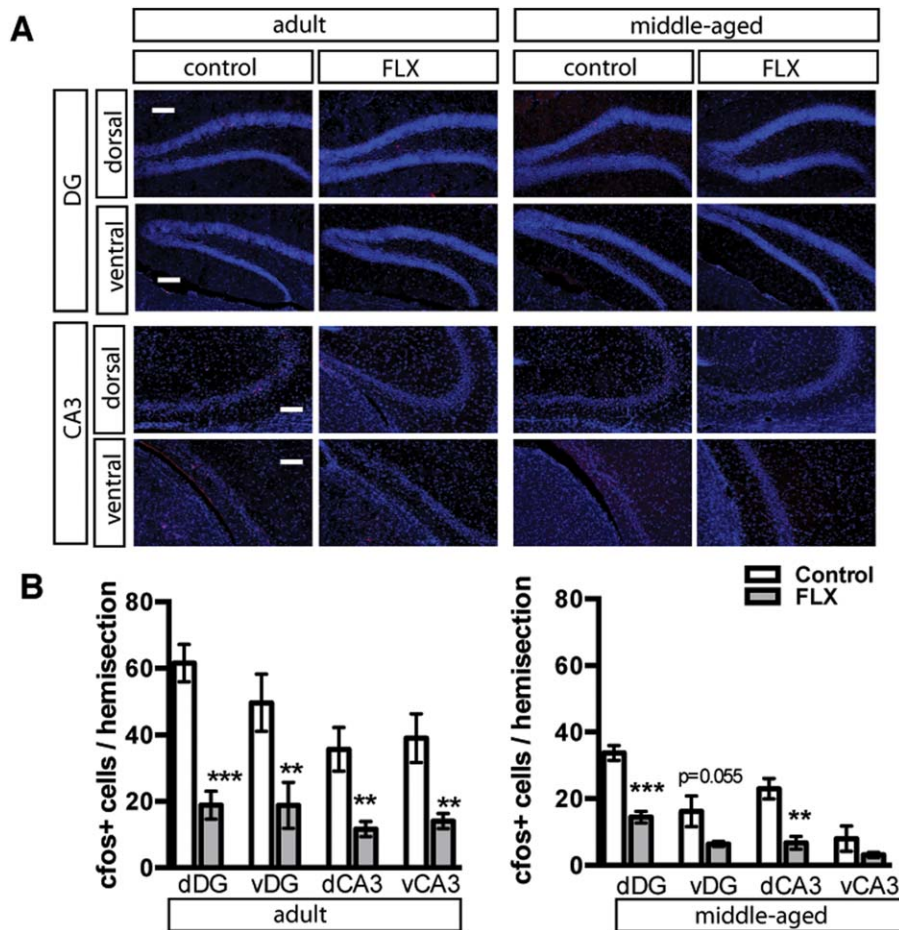
FIGURE 3.   Fluoxetine treatment decreases the basal expression of activity marker c-fos in DG and CA3 in adulthood and middle age. A. Representative cfos immunostained coronal sections of dorsal and ventral DG and CA3 in adult and middle-aged mice taken from home cage. Fluoxetine treatment 18mg/kg/day for 28 days. **B.** Quantification of c-fos positive cells. Adult $n = 3$ (VEH), 5 (FLX) mice per group, dDG $P = 0.0008$, vDG $P = 0.0326$, dCA3 $P = 0.0055$, vCA3 $P = 0.0067$; middle-aged $n = 3$ (VEH), 4 (FLX), dDG $P = 0.0009$, vDG $P = 0.0552$, dCA3 $P = 0.0052$, vCA3 $P = 0.1973$). Results are expressed as mean ($\pm$SEM). *$P < 0.05$; **$P < 0.01$; ***$P < 0.001$. Scale bar: 100 μM. [Color figure can be viewed in the online issue, which is available at wileyonlinelibrary.com.]

accompanied by a shift toward larger spines (Figure 5 C-D, MA $n = 3$ (VEH), 4 (FLX) dOML density $P = 0.0038$, distribution $P < 0.0001$).

To complement our analysis of dendritic spines of dentate granule neurons, we examined the effects of chronic fluoxetine treatment on mossy fibers in dorsal and ventral hippocampus of adult and middle-aged Thy-1 M GFP mice. Chronic fluoxetine treatment did not affect mossy fiber terminal size in dorsal hippocampus of adult or middle-aged mice (Figure 6A). However, middle-aged mice showed increased levels of the synaptic vesicle located zinc-transporter, ZnT3, in mossy fibers of ventral hippocampus (Figure 6B-C and left panel of D, MA $n = 3$ (VEH), 5 (FLX) $P = 0.0380$). Examination of immunoreactivity of the active zone marker, bassoon, did not reveal a change in mossy fiber active zones in adult mice or middle-aged mice, although a decrease in active zones was seen in the molecular layer of adult mice (Figure 6D (right panel), E-F, dML $P = 0.0274$, vML $P = 0.0525$).

Since CA1 is the major output of the hippocampus and receives inputs from CA3 as well as other brain regions, we used the same cohorts of Thy-1 M GFP mice to examine input specific changes in dendritic spines in the stratum oriens (SO), stratum radiatum (SR), and stratum lacunosum-moleculare (SLM) in response to chronic fluoxetine treatment. In both adult and middle-aged mice, we observed an increase in dendritic spine density in the stratum oriens, but not in the stratum radiatum or stratum lacunosum-moleculare of dorsal CA1 (Figure 7 A-E Adult $n = 3$ (VEH), 5 (FLX) dSO $P = 0.0490$, MA $n = 3$ (VEH), 4 (FLX) dSO $P = 0.0313$, vSO $P = 0.0461$). Middle-aged mice also showed an increase in spine size in the dorsal stratum lacunosom moleculare (Figure 7F, MA $n = 3$ (VEH), 4 (FLX) $P < 0.0001$). In contrast, in middle age, stratum radiatum of ventral CA1 showed an increase in dendritic spine density but a decrease in spine size (Figure 7 E, F MA $n = 3$ (VEH), 4 (FLX) density $P = 0.0505$, distribution $P = 0.0001$).
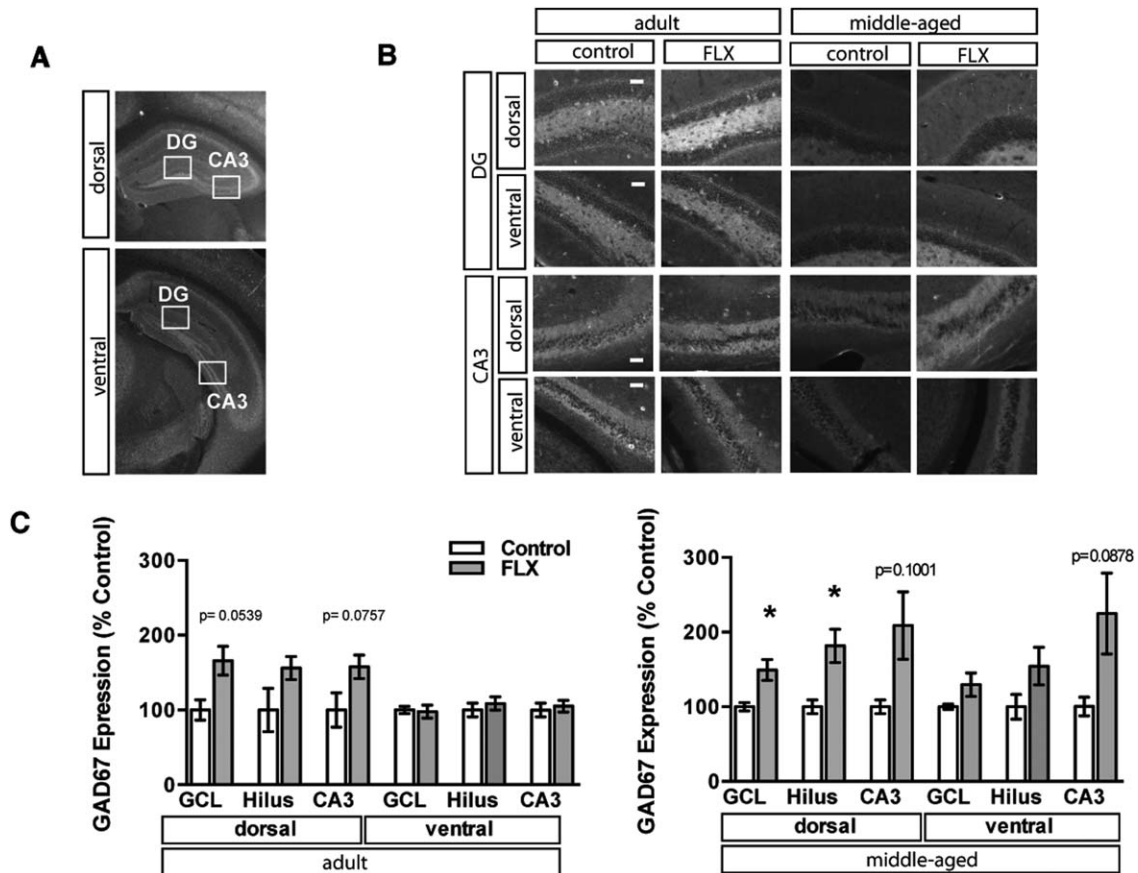
FIGURE 4. Fluoxetine treatment increases the expression of GAD67 in dorsal DG of middle-aged mice. A. Representative GAD67 immunostained dorsal and ventral coronal hippocampal sections of adult control mice. Boxes indicate approximate locations of high magnification micrographs in B. B. Representative high magnification images of GAD67 immunostained dorsal and ventral DG and CA3 from adult and middle-aged mice. Fluoxetine treatment 18 mg/kg/day for 28 days. C. GAD67 staining intensity was calculated from six hemisections per mouse (three dorsal, three ventral). Mean intensity (±SEM) is expressed as percent of control staining for matched region in age-matched controls. Adult $n = 3$ (VEH), 5 (FLX) mice per group, dGCL $P = 0.0539$, vGCL $P = 0.8602$, dHilus $P = 0.1065$, vHilus $P = 0.5456$, dCA3 $P = 0.0757$, vCA3 $P = 0.7003$; Middle-aged $n = 3$ (VEH), 4 (FLX), dGCL $P = 0.0351$, vGCL $P = 0.1423$, dHilus $P = 0.0309$, vHilus $P = 0.1464$, dCA3 $P = 0.1001$, vCA3 $P = 0.0878$). *$P < 0.05$. Scale bar: 50 µM.

As a first step toward assessing the impact of chronic fluoxetine treatment in middle-age on behavior, we examined hippocampal dependent learning and memory (contextual fear conditioning and memory precision), anxiety-like and depression-like behaviors. Middle-aged fluoxetine-treated animals exhibited normal locomotor activity (Figure 8A, no differences in total distance traveled in the open field; two-way repeated measures ANOVA, $n = 10$ (VEH), 10 (FLX); treatment $F_{(1,18)} = 0.9513$, $P = 0.3423$); but showed multiple indications of increased anxiety-like behavior. These include decreased exploratory behavior in the open field test (Figure 8B–D; decreased rearing behavior, Student's t-test; $n = 10$ (VEH), 10 (FLX), $P = 0.0094$; and decreased travel in the center of the open field (% distance in center; Student's t-test; $n = 10$ (VEH), 10 (FLX), $P = 0.0009$), the light dark test (decreased time in the light portion of the light–dark choice box; Student's t-test; $n = 10$ (VEH), 10 (FLX), $P = 0.0376$),

and the elevated plus maze (decreased time in the open arms; Student's t-test; $n = 10$ (VEH), 10 (FLX), $P = 0.0371$). No differences in anxiety behavior were observed in the novelty suppressed feeding test (no difference in latency to eat in the novel environment; Log-rank Mantel-Cox, $P = 0.8865$) Fluoxetine-treated animals exhibited a subtle anti-depressant-like response in the forced swim test (Figure 8 G; decreased time immobile on day 2 of the forced swim test (Student's t-test; $n = 10$ (VEH), 10 (FLX), $P = 0.0036$, but no difference in anhedonia (Figure 8F no difference in sucrose preference; two-way repeated measures ANOVA, $F_{(1,18)} = 0.4341$, $P = 0.5183$). To determine the impact of fluoxetine treatment on hippocampal-dependent learning, we assessed encoding and memory precision in a contextual fear conditioning task. Both groups of mice showed equivalent conditioning to the training context (Figure 8H; two-way repeated measures ANOVA, $n = 10$ (VEH), 10 (FLX), $F_{(1,18)} = 0.2154$, $P = 0.1594$), which
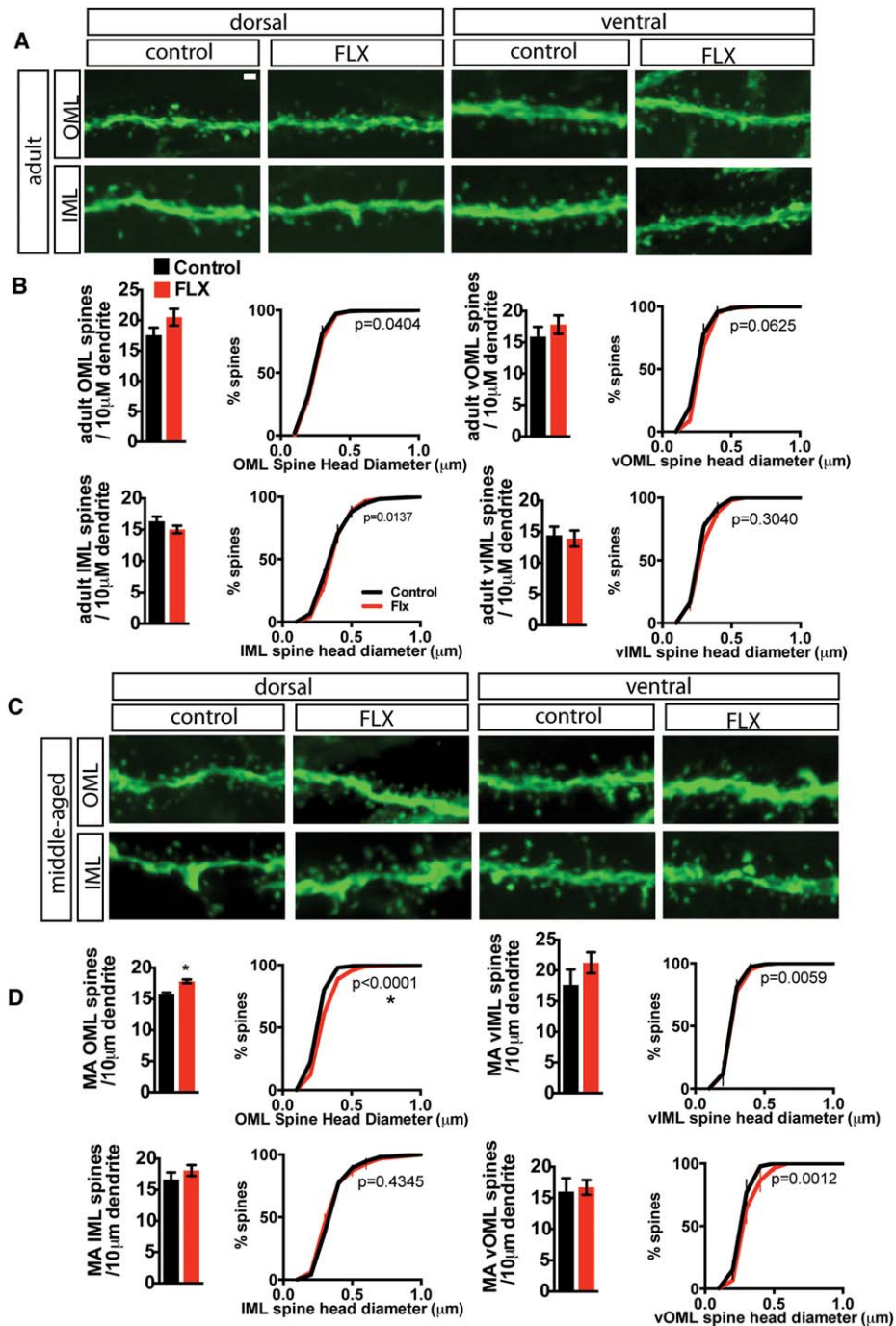
FIGURE 5.   Fluoxetine treatment increases the density of spines in the outer molecular layer in middle-aged mice. A. Representative high magnification micrographs of dorsal and ventral inner molecular layer (IML) and outer molecular layer (OML) dendritic segments from control and fluoxetine-treated (18 mg/kg/day for 28 days) adult *thy1-GFP* (M line) mice. **B.** Fluoxetine does not affect DG spine density or DG spine head diameter distribution for OML spines in dorsal (top left) and ventral (top right) DG or for IML in dorsal (bottom left) and ventral (bottom right) DG in adult mice. Data are expressed as mean (±SEM) number spines/10 µM dendrite (bar graphs). Student's *t*-test, $n = 3$, 5 (FLX) mice per group, dOML $P = 0.2009$, vOML $P = 0.4344$, dIML $P = 0.2354$, vIML $P = 0.7953$. Data is expressed as the group mean percentage (±SEM) as a function of size (Komolgrov-Smirnoff test $n = 3$ (VEH), 4 (FLX) mice, P values indicated on graphs with significance at $P = 0.0001$). **C.** Representative high magnification micrographs of dorsal and ventral inner molecular layer (IML) and outer molecular layer (OML) dendritic segments from control and fluoxetine treated middle-aged *thy1-GFP* (M line) mice. **D.** In middle-aged mice, fluoxetine increases dorsal OML spine density and shifts dOML spine head diameter distribution toward larger spines. Density and distribution data presented as in B. Student's *t*-test, $n = 3$ mice per group, dOML $P = 0.0038$, vOML $P = 0.7923$, dIML $P = 0.3665$. vIML $P = 0.3010$; *$P < 0.05$. P values for Komolgrov-Smirnoff test as indicated on graphs. Significance at $P \leq 0.0001$*). Scale bar 2: µM. [Color figure can be viewed in the online issue, which is available at wileyonlinelibrary.com.]
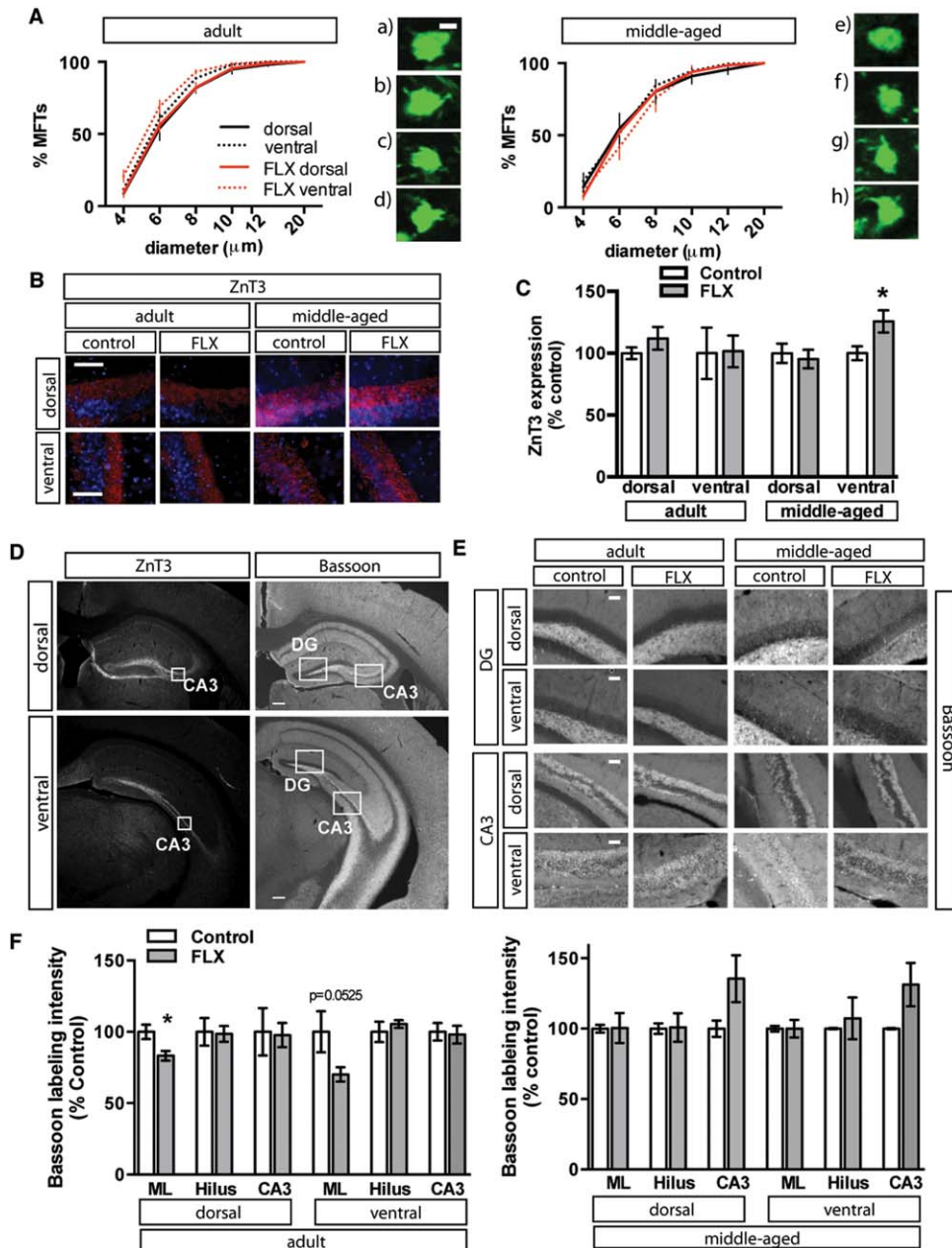
FIGURE 6.   Fluoxetine treatment does not alter the size distribution of Mossy fiber–CA3 synaptic terminals in adult or middle-aged mice A. Data are expressed as the group mean (±SEM) percentage as a function of size for adult (left) and middle-aged (right mice). Fluoxetine treatment 18 mg/kg/day for 28 days. Komolgrov-Smirnoff test adult $n = 3$ (VEH), 5 (FLX), adult dorsal $P = 0.4053$, adult ventral $P = 0.0256$, middle-aged ($n = 3$), MA dorsal $P = 0.1647$, MA ventral $P = 0.3670$. Significance at $P \leq 0.0001*$). Micrographs show representative mossy fiber terminals from (left) a) dorsal adult control, b) dorsal adult fluoxetine, c) ventral adult control, d) ventral adult fluoxetine and (right), e) dorsal MA control, f) dorsal MA fluoxetine, g) ventral MA control, h) ventral MA fluoxetine. B. Fluoxetine treatment results in increased ZnT3 in ventral hippocampus of middle-aged mice. Representative high magnification images of DAPI labeled ZnT3 immunostained dorsal and ventral CA3 from adult and middle-aged mice. C. ZnT3 staining intensity was calculated from six hemisections per mouse (three

dorsal, three ventral). D. Representative images of ZnT3 and Bassoon immunostaining in dorsal and ventral hippocampus of adult control mice. Boxes indicate approximate locations of high magnification micrographs in B and E. E. Representative high magnification images of Bassoon immunoreactivity in dorsal and ventral DG and CA3 from adult and middle-aged mice. Fluoxetine treated adult mice show decreased bassoon immunoreactivity in the molecular layer. F. Bassoon staining intensity was calculated from six hemisections per mouse (three dorsal, three ventral). Adult $n = 3$ (VEH), 5 (FLX) mice per group, dML $P = 0.0274$, vML $P = 0.0525$, dHilus $P = 0.8873$, vHilus $P = 0.4299$, dCA3 $P = 0.8939$, vCA3 $P = 0.8444$; middle-aged $n = 3$, 4 (FLX), dML $P = 0.9740$, vML $P = 0.9999$, dHilus $P = 0.9488$, vHilus $P = 0.6997$, dCA3 $P = 0.1412$, vCA3 $P = 0.1131* P < 0.05$. Scale bar: 2 μM (A), 50 μM (C), (E), 200 μM (D). Mean intensity (±SEM) is expressed as percent of control staining for age-matched controls. [Color figure can be viewed in the online issue, which is available at wileyonlinelibrary.com.]
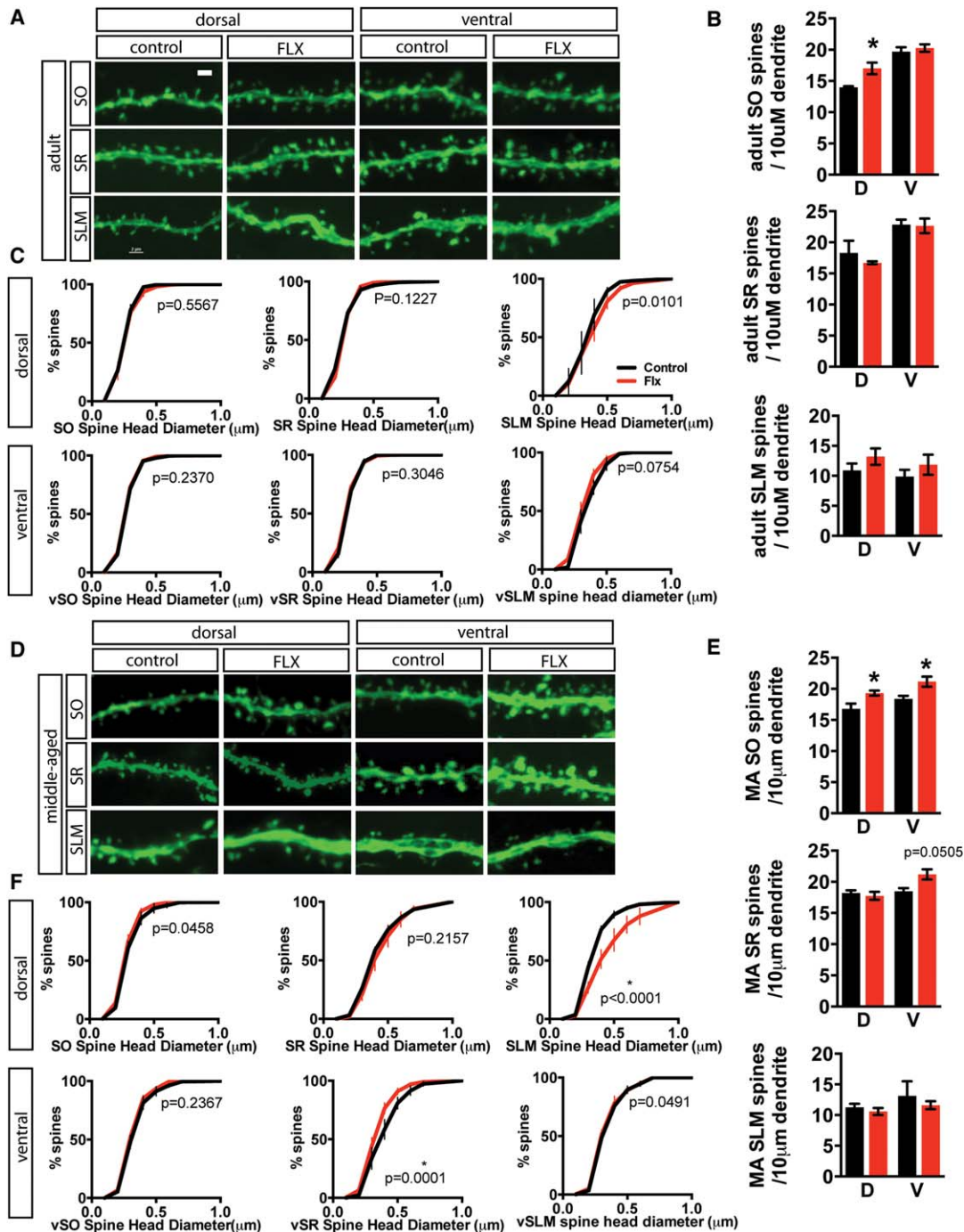
FIGURE 7. Fluoxetine treatment modifies CA1 dendritic spine density and spine head diameter in an age and laminae-specific manner. A. Representative high-magnification micrographs of dendritic segments in dorsal and ventral stratum oriens (SO), stratum radiatum (SR), and stratum lacunosum-moleculare (SLM) from control and fluoxetine-treated (18 mg/kg/day for 28 days) adult *thy1-GFP* (M line) mice. B, C. Fluoxetine treatment results in an increase in spine density in dorsal SO, but not in SR or SLM in adult mice. Data expressed as in Figure 5B. Student's *t*-test, adult *n* = 3, 5 (FLX) mice per group, dSO *P* = 0.0490, vSO *P* = 0.5655, dSR *P* = 0.3185, vSR *P* = 0.9134, dSLM *P* = 0.2902, vSLM *P* = 0.4345. For spine head diameter distribution, *P* values for Komolgrov-Smirnoff test as indicated on graphs. C. Representative high-magnification micrographs

of dendritic segments in dorsal and ventral stratum oriens (SO), stratum radiatum (SR), and stratum lacunosum-moleculare (SLM) from control and fluoxetine treated middle-aged *thy1-GFP* (M line) mice. D, E. Fluoxetine treatment results in an increase in spine density in dorsal SO, ventral SO, and ventral SR, while shifting spine size toward larger spines in dorsal SLM and toward smaller spines in ventral SR. Data expressed as in Figure 5B. Student's *t*-test, middle-aged *n* = 3 (VEH), 4 (FLX) mice per group, dSO *P* = 0.0313, vSO *P* = 0.0461, dSR *P* = 0.6100, vSR *P* = 0.0505, dSLM *P* = 0.4626, vSLM *P* = 0.5747; *P* < 0.05. For spine head diameter distribution, *P* values for Komolgrov-Smirnoff test as indicated on graphs. Scale bar: 2 μM. [Color figure can be viewed in the online issue, which is available at wileyonlinelibrary.com.]

was initially specific to this context as animals showed significantly less freezing in a similar context (Student's *t*-test; *n* = 10 (VEH), 10 (FLX), VEH A vs. B *P* < 0.0001, FLX A vs. B *P* < 0.0001). However, fluoxetine-treated animals showed a subtle enhancement of long-term memory precision as evidenced by improved discrimination between the training and safe context at two weeks following training (Student's *t*-test; *n* = 10 (VEH), 10 (FLX), VEH A vs. B *P* = 0.2448, FLX A vs. B *P* = 0.0243).

DISCUSSION

The widespread use of SSRIs for treatment of depression and anxiety disorders has motivated interrogation of a number of mechanistic changes potentially underlying therapeutic improvements, including changes in the connectivity and function of circuits in the prefrontal cortex, amygdala, hypothalamus, nucleus accumbens and hippocampus. In rodents, within the hippocampus, chronic fluoxetine treatment increases adult hippocampal neurogenesis (Malberg et al., 2000; Santarelli et al., 2003; Encinas et al., 2006; Sahay et al., 2007; David et al., 2009), directly modulates excitatory and inhibitory synaptic transmission (Stewart and Reid, 2000; Moutsimilli et al., 2005; Airan et al., 2007; Kobayashi et al., 2008, 2012; Reines et al., 2008; Luscher et al., 2011; Mendez et al., 2012; Rubio et al., 2013; Stagni et al., 2013), promotes dematuration of mature dentate granule neurons (Kobayashi et al., 2010), induces expression of growth factors and epigenetic changes (Berton and Nestler, 2006; Vialou et al., 2013), affects dendritic spines and dendritic complexity (Hajszan et al., 2005; Wang et al., 2008; Bessa et al., 2009; Huang et al., 2012; Rubio et al., 2013), and mossy fiber synaptic and structural plasticity (Kobayashi et al., 2008, 2010, 2012; Castren and Hen, 2013; Stagni et al., 2013). Studies investigating the causal relationships between this panoply of changes and therapeutic efficacy have implicated processes such as adult hippocampal neurogenesis and production of growth factors in some of the behavioral effects of fluoxetine in mouse models of depression (Schmidt and Duman, 2007; Miller and Hen, 2014).

In accord with recent studies, chronic fluoxetine treatment failed to enhance adult hippocampal neurogenesis in middle age rodents (Cowen et al., 2008; Couillard-Despres et al., 2009; Guirado et al., 2012). The lack of an effect on proliferation of neural stem cells and progenitors and survival of adult-born neurons in middle age may reflect a cell-autonomous loss in competence to respond to serotonergic signaling, thereby requiring a higher dose of fluoxetine to promote adult hippocampal neurogenesis, or may reflect changes in niche agencies such as interneurons and mature dentate granule neurons that regulate proliferation and survival through secretion of growth factors and neural activity. Alternatively, chronic fluoxetine may act by preventing the decrease in adult hippocampal neurogenesis that is seen with chronic stress (Tanti et al., 2013) or by

enhancing neurogenesis when exposed to stressors such as chronic corticosterone (David et al., 2009).

In contrast to the age-dependence of fluoxetine's pro-neurogenic effects, chronic fluoxetine treatment promoted dematuration of dentate granule neurons in adulthood and in middle age. Consistent with previous reports (Kobayashi et al., 2010), this de-differentiation was accompanied by a profound reduction in activity-dependent gene expression in DG and CA3 as assessed by c-fos immunohistochemistry. Reduction in calbindin expression in the DG is associated with altered excitation-inhibition balance (Palop et al., 2003) and administration of valproic acid, an anticonvulsant, has been shown to reverse dematuration of the DG in specific mouse mutants (Hagihara et al., 2013). Whether changes in excitation-inhibition balance in the dentate gyrus or dematuration of dentate granule neurons are critically required for the antidepressant actions of fluoxetine are yet to be determined.

An important unaddressed question hampering our understanding of potential links between hippocampal circuitry changes and pertinent antidepressant responses is the lack of data on how specific hippocampal microcircuits are changed by chronic fluoxetine treatment. Fluoxetine-induced changes in dendritic inputs within specific DG and CA1 laminae may contribute to the therapeutic response by impacting information processing in these regions. Analysis of dendritic spines in the inner molecular layer and outer molecular layer of the dorsal and ventral DG in adult and middle-aged mice did not reveal any changes in density or distribution following fluoxetine treatment, with the notable exception of the outer molecular layer of the middle-age dorsal DG. The lack of an effect of fluoxetine treatment on dendritic spines of mature dentate granule neurons in adulthood is consistent with a previous report that used golgi staining to analyze spine density (Bessa et al., 2009). However, our study specifically addressed the inputs onto mature neurons without the potential confounding contribution of young neurons of varying maturity. These results suggest that, at least in the DG, chronic fluoxetine treatment in adulthood does not stimulate spine formation, though it may protect from spine loss under conditions of chronic stress. Furthermore, since our study examines a single snapshot in time, it does not address the possibility that fluoxetine treatment changes the rate of spine turnover as suggested by a recent study looking at remodeling of interneuron branch tips in the visual cortex (Chen et al., 2011).

Examination of dendritic spines of CA1 pyramidal neurons, the principal output neurons of the hippocampus, revealed an increase in dendritic spine density of basal dendrites in adulthood and middle age following fluoxetine treatment. There is growing evidence to suggest that basal and apical dendrites of CA1 have different properties, including excitability and therefore, may differentially contribute to information processing (Spruston, 2008). For example, basal dendrites have a lower threshold for long-term potentiation (Kaibara and Leung, 1993; Leung and Shen, 1995) and exhibit higher synaptic transmission during theta states than apical dendrites (Leung and Peloquin, 2010). Furthermore, basal dendrites of CA1

pyramidal neurons show greater dopaminergic modulation (Li et al., in press) and lower cholinergic attenuation of synaptic transmission than apical dendrites (Leung and Peloquin, 2010). Importantly, spatial learning exerts a greater increase in dendritic spine density of basal dendrites (Moser et al., 1997; Gonzalez-Ramirez et al., 2014; Harland et al., 2014). Whether these properties of basal dendrites are changed following chronic fluoxetine is not known.

While the basis for the heightened sensitivity of dendritic spines of basal dendrites in CA1 and OML dendritic regions in the DG to fluoxetine is not known, these changes may reflect differential serotonin-dependent modulation of upstream principle input cells, local inhibitory control, or differential sensitivity of pre- or post-synaptic cells to serotonin levels. The

OML, but not IML, receives inputs from layer II cells of the enthorinal cortex, which are hyperpolarized by serotonin (Lei, 2012). CA3 neurons further away from CA1 project primarily to apical dendrites, whereas CA3 neurons more proximal to CA1 project preferentially to basal dendrites (Ishizuka et al., 1990; Li et al., 1994). All seven classes of serotonin receptors are expressed in the hippocampus in a range of cell-types and in a laminae-specific distribution along the septotemporal axis (Berumen et al., 2012; Tanaka et al., 2012). These receptors can have excitatory or inhibitory effects on granule and pyramidal neurons or on interneurons (Pytliak et al., 2011), and may thereby act to fine-tune dendritic spine plasticity. For example, excitatory inputs from CA3 to CA1 pyramidal neurons are enhanced by serotonin receptor 7 and inhibited by serotonin
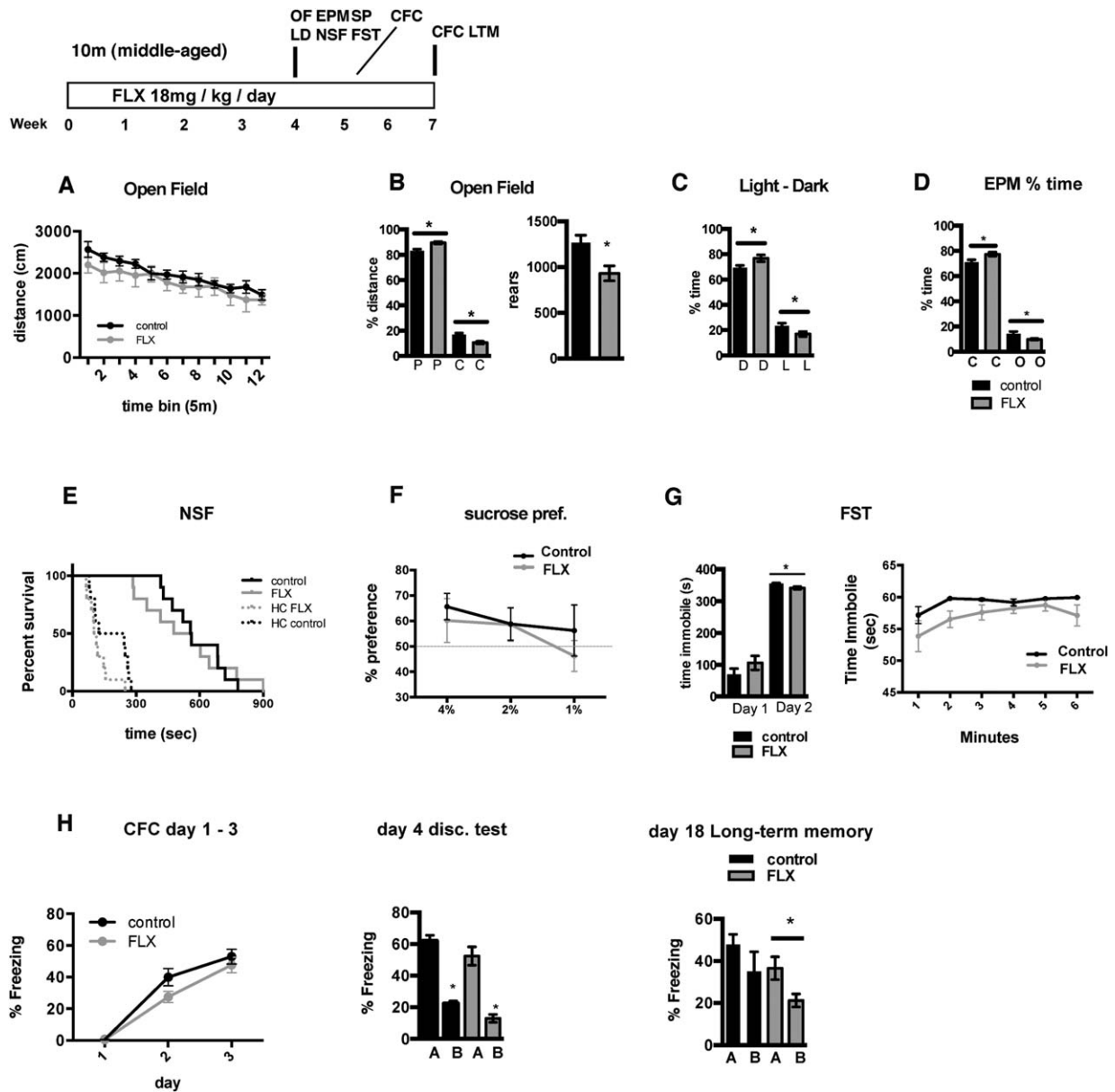

FIGURE 8.

1A receptors (Berumen et al., 2012). In addition, the ventral DG receives greater serotonergic innervation and expresses higher levels of serotonin 1A receptor than the dorsal DG and dorsal CA1 expresses higher levels of this receptor than ventral CA1 (Gage and Thompson, 1980; Ihara et al., 1988; Tanaka et al., 2012).

Notably, our analysis revealed that multiple factors in the DG (calbindin, GAD67, and mossy fiber terminal ZnT3 expression, dendritic spine density, and distribution in the OML), and in CA1 (dendritic spine density in dSO, vSO, vSR, and distribution in vSR, SLM) display increased sensitivity to chronic fluoxetine in middle age. It may be that changes in pattern of innervation and receptor expression in middle age underlie this increased sensitivity to chronic fluoxetine. Interestingly, a study using middle-aged mice suggests that hippocampal levels of serotonin receptor 7 decrease from adulthood to middle-age while serotonin receptor 1A expression increases (Saroja et al., 2014). A study in aged rats found unchanged serotonin receptor 1A expression at baseline, but decreased response of serotonin receptor 1A expression in response to the antidepressant amitriptyline in the dorsal raphe, which may decrease autoregulation and hence increase serotonergic signaling (Yau et al., 1999). Furthermore, aged humans show higher serum concentrations of fluoxetine than adults (Reis et al., 2009), which may yield increased sensitivity. Together, the analysis of dendritic spines in adulthood and middle age suggest an increased sensitivity of the middle-aged hippocampus to fluoxetine- dependent spine remodeling. A complimentary explanation is that there is age-dependent accumulation of "cytoskeletal brakes," which, when relieved by fluoxetine, results in greater synaptic remodeling (Bloss et al., 2010). The molecular identities of these brakes are however unclear.

How the fluoxetine-induced changes in the middle-aged DG influence computations in the hippocampus such as pattern separation and pattern completion to govern antidepressant responses is not known (Sahay and Hen, 2007). To begin to understand how the fluoxetine-induced cellular and molecular changes in middle-age impact behavior, we examined the effects of chronic fluoxetine treatment on anxiety-like behavior, depression-like behavior, and hippocampus dependent learning and memory in female middle-aged mice. Our results suggest that fluoxetine treatment significantly increases anxiety-like behavior in multiple tests, antidepressant-like behavioral response in the forced swim test and precision of long-term contextual fear memory. Further studies will be necessary to probe causal relationships between fluoxetine-induced changes in input-specific synapse remodeling and cellular and circuit-plasticity with neural mechanisms such as pattern separation and behavior in adulthood and throughout aging. In addition, it will be particularly valuable to examine the relationships between these changes in the context of mouse models of depression.

In conclusion, our studies identify a constellation of cellular and structural changes induced by chronic fluoxetine along the septotemporal axis of the DG and CA1 in adulthood and in middle age. Together these data help generate a framework for understanding how changes in input-specific connectivity mesh with previously described changes in inhibition, dematuration of dentate granule neurons, and adult hippocampal neurogenesis to influence encoding functions of the hippocampus and, ultimately, to determine whether these changes are necessary in mediating adaptive behavioral responses of fluoxetine under conditions of chronic stress in adulthood and middle age.

FIGURE 8.   Fluoxetine treatment in middle-aged mice leads to increased anxiety-like and antidepressant-like behaviors and enhances precision of long-term contextual fear memory. A. Distance traveled over time in the open field enclosure is not significantly different between control and fluoxetine-treated (18 mg/kg/day for 28 days) middle-aged C57Bl/6 mice (two-way repeated measures ANOVA, n = 10 (VEH), 10 (FLX); Interaction ($F_{(11,198)} = 0.5998$) P = 0.8277, time ($F_{(11,198)} = 16.63$) $P <$ 0.0001, Treatment ($F_{(1,18)} = 0.9513$) P = 0.3423). B. Fluoxetine-treated mice exhibit a decrease in percentage of distance traveled in the center (C) of the open field (left graph; periphery (P)). Student's t-test, n = 10 (VEH), 10 (FLX); center P = 0.0009, periphery P = 0.0009. Fluoxetine-treated mice show fewer rearing events in 1hr in the open field enclosure (right graph). Student's t-test, n = 10 (VEH), 10 (FLX); P = 0.0094. C. Fluoxetine-treated mice spend a smaller percentage of time in the light (L) compartment of the light-dark choice apparatus (D = dark compartment). Student's t-test, n = 10 (VEH), 10 (FLX); light P = 0.0376, dark P = 0.0307. D. Fluoxetine-treated mice spend a smaller percentage of time in the open arms (O) of the elevated plus maze apparatus (c = closed arms). Student's t-test, n = 10 (VEH), 10 (FLX); open P = 0.0371, closed P = 0.024. E. Latency to consume food is not different between control and Fluoxetine-treated mice in either the novel area or the home cage (HC) in the novelty-suppressed feeding test (Log-rank Mantel-Cox test, n = 10 (VEH), 10 (FLX); novel P = 0.8865, HC P = 0.0706). F. Sucrose preference (volume sucrose/total volume sucrose + water) does not differ between control and Fluoxetine-treated mice at any tested sucrose concentration (1, 2, or 4%) (two-way repeated measures ANOVA, n = 10 (VEH), 10 (FLX); interaction ($F_{(2,36)} = 0.3584$) P = 0.7012, sucrose % ($F_{(2,36)} = 2.120$) $P <$ 0.1348, Trt ($F_{(1,18)} = 0.4341$) P = 0.5183). G. Fluoxetine-treated mice spend less time immobile than control mice on day 2 of the forced swim test (left graph; Student's t-test, n = 10 (VEH), 10 (FLX); day 1 P = 0.2198, day 2 P = 0.0036. Right graph time immobile by minute on test on day 2; two-way repeated measures ANOVA, n = 10 (VEH), 10 (FLX) per group α = 0.05; interaction ($F_{(5,80)} = 0.5825$) P = 0.7133, time ($F_{(5,80)} = 3.573$) P = 0.0057, treatment ($F_{(1,16)} = 9.465$) P = 0.0072. H. Acquisition of freezing behavior is not significantly different between control and fluoxetine-treated middle-aged C57Bl/6 mice (left graph; two-way repeated measures ANOVA, n = 10 (VEH), 10 (FLX) per group α = 0.05; interaction ($F_{(2,36)} = 1.974$) P = 0.1536, day ($F_{(2,36)} = 131.9$) $P <$ 0.0001, treatment ($F_{(1,18)} = 2.154$) P = 0.1594). Discrimination of the shock context and novel, safe context does not differ between control and fluoxetine treated mice (center graph). Student's t-test, n = 10 (VEH), 10 (FLX); VEH A vs. VEH B $P <$ 0.0001, FLX A vs. FLX B $P <$ 0.0001. Fluoxetine-treated middle-aged mice show a subtle enhancement in discrimination of the shock context and safe context at 2 weeks following the initial discrimination test (right graph; Student's t-test, n = 10 (VEH), 10 (FLX); VEH A vs. VEH B P = 0.2448, FLX A vs. FLX B P = 0.0243).

Acknowledgments

AUTHOR CONTRIBUTIONS

REFERENCES

Airan RD, Meltzer LA, Roy M, Gong Y, Chen H, Deisseroth K. 2007. High-speed imaging reveals neurophysiological links to behavior in an animal model of depression. Science 317:819–823.

Amaral DG, Scharfman HE, Lavenex P. 2007. The dentate gyrus: Fundamental neuroanatomical organization (dentate gyrus for dummies). Prog Brain Res 163:3–22.

Berton O, Nestler EJ. 2006. New approaches to antidepressant drug discovery: Beyond monoamines. Nat Rev Neurosci 7:137–151.

Berumen LC, Rodriguez A, Miledi R, Garcia-Alcocer G. 2012. Serotonin receptors in hippocampus. Sci World J 2012:823493.

Bessa JM, Ferreira D, Melo I, Marques F, Cerqueira JJ, Palha JA, Almeida OF, Sousa N. 2009. The mood-improving actions of antidepressants do not depend on neurogenesis but are associated with neuronal remodeling. Mol Psychiatry 14:764-773, 739.

Bloss EB, Janssen WG, McEwen BS, Morrison JH. 2010. Interactive effects of stress and aging on structural plasticity in the prefrontal cortex. J Neurosci 30:6726–6731.

Bosch M, Hayashi Y. 2012. Structural plasticity of dendritic spines. Curr Opin Neurobiol 22:383–388.

Castren E, Hen R. 2013. Neuronal plasticity and antidepressant actions. Trends Neurosci 36:259–267.

Chen F, Madsen TM, Wegener G, Nyengaard JR. 2008. Changes in rat hippocampal ca1 synapses following imipramine treatment. Hippocampus 18:631–639.

Chen JL, Lin WC, Cha JW, So PT, Kubota Y, Nedivi E. 2011. Structural basis for the role of inhibition in facilitating adult brain plasticity. Nat Neurosci 14:587–594.

Conti B, Maier R, Barr AM, Morale MC, Lu X, Sanna PP, Bilbe G, Hoyer D, Bartfai T. 2007. Region-specific transcriptional changes following the three antidepressant treatments electro convulsive therapy, sleep deprivation and fluoxetine. Mol Psychiatry 12:167–189.

Couillard-Despres S, Wuertinger C, Kandasamy M, Caioni M, Stadler K, Aigner R, Bogdahn U, Aigner L. 2009. Ageing abolishes the effects of fluoxetine on neurogenesis. Mol Psychiatry 14:856–864.

Cowen DS, Takase LF, Fornal CA, Jacobs BL. 2008. Age-dependent decline in hippocampal neurogenesis is not altered by chronic treatment with fluoxetine. Brain Res 1228:14–19.

David DJ, Samuels BA, Rainer Q, Wang JW, Marsteller D, Mendez I, Drew M, Craig DA, Guiard BP, Guilloux JP, Artymyshyn RP, Gardier AM, Gerald C, Antonijevic IA, Leonardo ED, Hen R. 2009. Neurogenesis-dependent and -independent effects of fluoxetine in an animal model of anxiety/depression. Neuron 62:479–493.

Encinas JM, Vaahtokari A, Enikolopov G. 2006. Fluoxetine targets early progenitor cells in the adult brain. Proc Natl Acad Sci USA 103:8233–8238.

Eriksson PS, Perfilieva E, Bjork-Eriksson T, Alborn AM, Nordborg C, Peterson DA, Gage FH. 1998. Neurogenesis in the adult human hippocampus. Nat Med 4:1313–1317.

Fanselow MS, Dong HW. 2010. Are the dorsal and ventral hippocampus functionally distinct structures? Neuron 65:7–19.

Feng G, Mellor RH, Bernstein M, Keller-Peck C, Nguyen QT, Wallace M, Nerbonne JM, Lichtman JW, Sanes JR. 2000. Imaging neuronal subsets in transgenic mice expressing multiple spectral variants of GFP. Neuron 28:41–51.

Gage FH, Thompson RG. 1980. Differential distribution of norepinephrine and serotonin along the dorsal-ventral axis of the hippocampal formation. Brain Res Bull 5:771–773.

Gonzalez-Ramirez MM, Velazquez-Zamora DA, Olvera-CME, Gonzalez-Burgos I. 2014. Changes in the plastic properties of hippocampal dendritic spines underlie the attenuation of place learning in healthy aged rats. Neurobiol Learn Mem 109:94–103.

Guirado R, Sanchez-Matarredona D, Varea E, Crespo C, Blasco-Ibanez JM, Nacher J. 2012. Chronic fluoxetine treatment in middle-aged rats induces changes in the expression of plasticity-related molecules and in neurogenesis. BMC Neuroscience 13:5.

Guirado R, Perez-Rando M, Sanchez-Matarredona D, Castren E, Nacher J. 2014. Chronic fluoxetine treatment alters the structure, connectivity and plasticity of cortical interneurons. Int J Neuropsychopharmacol 17:1635–1646.

Hagihara H, Takao K, Walton NM, Matsumoto M, Miyakawa T. 2013. Immature dentate gyrus: An endophenotype of neuropsychiatric disorders. Neural Plasticity 2013:318596.

Hajszan T, MacLusky NJ, Leranth C. 2005. Short-term treatment with the antidepressant fluoxetine triggers pyramidal dendritic spine synapse formation in rat hippocampus. Eur J Neurosci 21:1299–1303.

Harland BC, Collings DA, McNaughton N, Abraham WC, Dalrymple-Alford JC. 2014. Anterior thalamic lesions reduce spine density in both hippocampal ca1 and retrosplenial cortex, but enrichment rescues ca1 spines only. Hippocampus 24:1232–1247.

Huang GJ, Ben-David E, Tort Piella A, Edwards A, Flint J, Shifman S. 2012. Neurogenomic evidence for a shared mechanism of the antidepressant effects of exercise and chronic fluoxetine in mice. PLoS One 7:e35901.

Ihara N, Ueda S, Kawata M, Sano Y. 1988. Immunohistochemical demonstration of serotonin-containing nerve fibers in the mammalian hippocampal formation. Acta Anat 132:335–346.

Ikrar T, Guo N, He K, Besnard A, Levinson S, Hill A, Lee HK, Hen R, Xu X, Sahay A. 2013. Adult neurogenesis modifies excitability of the dentate gyrus. Front Neural Circuits 7:204.

Ishizuka N, Weber J, Amaral DG. 1990. Organization of intrahippocampal projections originating from ca3 pyramidal cells in the rat. J Comp Neurol 295:580–623.

Kaibara T, Leung LS. 1993. Basal versus apical dendritic long-term potentiation of commissural afferents to hippocampal ca1: A current-source density study. J Neurosci 13:2391–2404.

Knoth R, Singec I, Ditter M, Pantazis G, Capetian P, Meyer RP, Horvat V, Volk B, Kempermann G. 2010. Murine features of neurogenesis in the human hippocampus across the lifespan from 0 to 100 years. PLoS One 5:e8809.

Kobayashi K, Ikeda Y, Haneda E, Suzuki H. 2008. Chronic fluoxetine bidirectionally modulates potentiating effects of serotonin on the hippocampal mossy fiber synaptic transmission. J Neurosci 28:6272–6280.

Kobayashi K, Ikeda Y, Sakai A, Yamasaki N, Haneda E, Miyakawa T, Suzuki H. 2010. Reversal of hippocampal neuronal maturation by serotonergic antidepressants. Proc Natl Acad Sci USA 107:8434–8439.

Kobayashi K, Haneda E, Higuchi M, Suhara T, Suzuki H. 2012. Chronic fluoxetine selectively upregulates dopamine D(1)-like receptors in the hippocampus. Neuropsychopharmacology 37: 1500–1508.

Lei S. 2012. Serotonergic modulation of neural activities in the entorhinal cortex. Int J Physiol Pathophysiol Pharmacol 4:201–210.

Leranth C, Hajszan T. 2007. Extrinsic afferent systems to the dentate gyrus. Prog Brain Res 163:63–84.

Lesch KP, Waider J. 2012. Serotonin in the modulation of neural plasticity and networks: Implications for neurodevelopmental disorders. Neuron 76:175–191.

Leung LS, Peloquin P. 2010. Cholinergic modulation differs between basal and apical dendritic excitation of hippocampal ca1 pyramidal cells. Cereb Cortex 20:1865–1877.

Leung LS, Shen B. 1995. Long-term potentiation at the apical and basal dendritic synapses of ca1 after local stimulation in behaving rats. J Neurophysiol 73:1938–1946.

Li SB, Du D, Hasan MT, Kohr G. D4 receptor activation differentially modulates hippocampal basal and apical dendritic synapses in freely moving mice. Cereb Cortex 2014 Sep 30. [Epub ahead of print]

Li XG, Somogyi P, Ylinen A, Buzsaki G. 1994. The hippocampal ca3 network: An in vivo intracellular labeling study. J Comp Neurol 339:181–208.

Li Y, Luikart BW, Birnbaum S, Chen J, Kwon CH, Kernie SG, Bassel-Duby R, Parada LF. 2008. TrkB regulates hippocampal neurogenesis and governs sensitivity to antidepressive treatment. Neuron 59:399–412.

Luscher B, Shen Q, Sahir N. 2011. The GABAergic deficit hypothesis of major depressive disorder. Mol Psychiatry 16:383–406.

Malberg JE, Eisch AJ, Nestler EJ, Duman RS. 2000. Chronic antidepressant treatment increases neurogenesis in adult rat hippocampus. J Neurosci 20:9104–9110.

Mateus-Pinheiro A, Pinto L, Bessa JM, Morais M, Alves ND, Monteiro S, Patricio P, Almeida OF, Sousa N. 2013. Sustained remission from depressive-like behavior depends on hippocampal neurogenesis. Transl Psychiatry 3:e210.

Mendez P, Pazienti A, Szabo G, Bacci A. 2012. Direct alteration of a specific inhibitory circuit of the hippocampus by antidepressants. J Neurosci 32:16616–16628.

Miller BH, Schultz LE, Gulati A, Cameron MD, Pletcher MT. 2008. Genetic regulation of behavioral and neuronal responses to fluoxetine. Neuropsychopharmacology 33:1312–1322.

Miller BR, Hen R. 2014. The current state of the neurogenic theory of depression and anxiety. Curr Opin Neurobiol 30:51–58. C:

Miller RA, Harrison DE, Astle CM, Floyd RA, Flurkey K, Hensley KL, Javors MA, Leeuwenburgh C, Nelson JF, Ongini E, Nadon NL, Warner HR, Strong R. 2007. An aging interventions testing program: Study design and interim report. Aging Cell 6:565–575.

Moser MB, Trommald M, Egeland T, Andersen P. 1997. Spatial training in a complex environment and isolation alter the spine distribution differently in rat ca1 pyramidal cells. J Comp Neurol 380:373–381.

Moutsimilli L, Farley S, Dumas S, El Mestikawy S, Giros B, Tzavara ET. 2005. Selective cortical vglut1 increase as a marker for antidepressant activity. Neuropharmacology 49:890–900.

O'Leary OF, Cryan JF. 2014. A ventral view on antidepressant action: Roles for adult hippocampal neurogenesis along the dorsoventral axis. Trends Pharmacol Sci 35:675–687.

Palop JJ, Jones B, Kekonius L, Chin J, Yu GQ, Raber J, Masliah E, Mucke L. 2003. Neuronal depletion of calcium-dependent proteins in the dentate gyrus is tightly linked to Alzheimer's disease-related cognitive deficits. Proc Natl Acad Sci USA 100:9572–9577.

Patricio P, Mateus-Pinheiro A, Irmler M, Alves ND, Machado-Santos AR, Morais M, Correia JS, Korostynski M, Piechota M, Stoffel R, Beckers J, Bessa JM, Almeida OF, Sousa N, Pinto L. 2015. Differential and converging molecular mechanisms of antidepressants'

action in the hippocampal dentate gyrus. Neuropsychopharmacology 40:338–349.

Paxinos G, Franklin KBJ. 2004. The Mouse Brain in Stereotaxic Coordinates: Compact, 2nd ed. San Diego, CA: Elsevier Academic Press.

Pittenger C, Duman RS. 2008. Stress, depression, and neuroplasticity: A convergence of mechanisms. Neuropsychopharmacology 33:88–109.

Pytliak M, Vargova V, Mechirova V, Felsoci M. 2011. Serotonin receptors - From molecular biology to clinical applications. Physiol Res 60:15–25.

Reines A, Cereseto M, Ferrero A, Sifonios L, Podesta MF, Wikinski S. 2008. Maintenance treatment with fluoxetine is necessary to sustain normal levels of synaptic markers in an experimental model of depression: Correlation with behavioral response. Neuropsychopharmacology 33:1896–1908.

Reis M, Aamo T, Spigset O, Ahlner J. 2009. Serum concentrations of antidepressant drugs in a naturalistic setting: Compilation based on a large therapeutic drug monitoring database. Ther Drug Monitor 31:42–56.

Rubio FJ, Ampuero E, Sandoval R, Toledo J, Pancetti F, Wyneken U. 2013. Long-term fluoxetine treatment induces input-specific LTP and LTD impairment and structural plasticity in the ca1 hippocampal subfield. Front Cell Neurosci 7:66.

Sahay A, Hen R. 2007. Adult hippocampal neurogenesis in depression. Nat Neurosci 10:1110–1115.

Sahay A, Drew MR, Hen R. 2007. Dentate gyrus neurogenesis and depression. Prog Brain Res 163:697–722.

Santarelli L, Saxe M, Gross C, Surget A, Battaglia F, Dulawa S, Weisstaub N, Lee J, Duman R, Arancio O, Belzung C, Hen R. 2003. Requirement of hippocampal neurogenesis for the behavioral effects of antidepressants. Science 301:805–809.

Saroja SR, Kim EJ, Shanmugasundaram B, Hoger H, Lubec G. 2014. Hippocampal monoamine receptor complex levels linked to spatial memory decline in the aging C57BL/6J. Behav Brain Res 264:1–8.

Schmidt HD, Duman RS. 2007. The role of neurotrophic factors in adult hippocampal neurogenesis, antidepressant treatments and animal models of depressive-like behavior. Behav Pharmacol 18:391–418.

Shirayama Y, Chen AC, Nakagawa S, Russell DS, Duman RS. 2002. Brain-derived neurotrophic factor produces antidepressant effects in behavioral models of depression. J Neurosci 22:3251–3261.

Snyder JS, Cameron HA. 2012. Could adult hippocampal neurogenesis be relevant for human behavior? Behav Brain Res 227:384–390.

Snyder JS, Ramchand P, Rabbett S, Radik R, Wojtowicz JM, Cameron HA. 2011. Septotemporal gradients of neurogenesis and activity in 13-month-old rats. Neurobiol Aging 32:1149–1156.

Spalding KL, Bergmann O, Alkass K, Bernard S, Salehpour M, Huttner HB, Bostrom E, Westerlund I, Vial C, Buchholz BA, Possnert G, Mash DC, Druid H, Frisen J. 2013. Dynamics of hippocampal neurogenesis in adult humans. Cell 153:1219–1227.

Spruston N. 2008. Pyramidal neurons: Dendritic structure and synaptic integration. Nat Rev Neurosci 9:206–221.

Stagni F, Magistretti J, Guidi S, Ciani E, Mangano C, Calza L, Bartesaghi R. 2013. Pharmacotherapy with fluoxetine restores functional connectivity from the dentate gyrus to field ca3 in the Ts65Dn mouse model of down syndrome. PLoS One 8:e61689.

Stewart CA, Reid IC. 2000. Repeated ECS and fluoxetine administration have equivalent effects on hippocampal synaptic plasticity. Psychopharmacology (Berl) 148:217–223.

Strange BA, Witter MP, Lein ES, Moser EI. 2014. Functional organization of the hippocampal longitudinal axis. Nat Rev Neurosci 15:655–669.

Surget A, Tanti A, Leonardo ED, Laugeray A, Rainer Q, Touma C, Palme R, Griebel G, Ibarguen-Vargas Y, Hen R, Belzung C. 2011. Antidepressants recruit new neurons to improve stress response regulation. Mol Psychiatry 16:1177–1188.

Tanaka KF, Samuels BA, Hen R. 2012. Serotonin receptor expression along the dorsal-ventral axis of mouse hippocampus. Philos Trans R Soc Lond 367:2395–2401.

Tanti A, Westphal WP, Girault V, Brizard B, Devers S, Leguisquet AM, Surget A, Belzung C. 2013. Region-dependent and stage-specific effects of stress, environmental enrichment, and antidepressant treatment on hippocampal neurogenesis. Hippocampus 23:797–811.

Vialou V, Feng J, Robison AJ, Nestler EJ. 2013. Epigenetic mechanisms of depression and antidepressant action. Annu Rev Pharmacol Toxicol 53:59–87.

Vuksic M, Del Turco D, Bas Orth C, Burbach GJ, Feng G, Muller CM, Schwarzacher SW, Deller T. 2008. 3D-reconstruction and functional properties of GFP-positive and GFP-negative granule cells in the fascia dentata of the Thy1-GFP mouse. Hippocampus 18:364–375.

Walker AK, Rivera PD, Wang Q, Chuang JC, Tran S, Osborne-Lawrence S, Estill SJ, Starwalt R, Huntington P, Morlock L, Naidoo J, Williams NS, Ready JM, Eisch AJ, Pieper AA, Zigman JM. In press. The p7c3 class of neuroprotective compounds exerts antidepressant efficacy in mice by increasing hippocampal neurogenesis. Mol Psychiatry 2015;20:500–508.

Wang JW, David DJ, Monckton JE, Battaglia F, Hen R. 2008. Chronic fluoxetine stimulates maturation and synaptic plasticity of adult-born hippocampal granule cells. J Neurosci 28:1374–1384.

Wu MV, Hen R. 2014. Functional dissociation of adult-born neurons along the dorsoventral axis of the dentate gyrus. Hippocampus 24:751–761.

Yau JL, Kelly PA, Olsson T, Noble J, Seckl JR. 1999. Chronic amitriptyline administration increases serotonin transporter binding sites in the hippocampus of aged rats. Neurosci Lett 261:183–185.